

Fluorine incorporation into calcite, aragonite and vaterite CaCO_3 : Computational chemistry insights and geochemistry implications

Xiaolei Feng^{a,b}, Zvi Steiner^{c,b,*}, Simon A. T. Redfern^{d,*}

^a*Institute for Disaster Management and Reconstruction, Sichuan University - Hong Kong Polytechnic University, Chengdu, 610207, China*

^b*Department of Earth Sciences, University of Cambridge, Downing Street, Cambridge, CB2 3EQ, UK*

^c*GEOMAR Helmholtz Centre for Ocean Research, Kiel, 24105 Germany*

^d*Asian School of the Environment, Nanyang Technological University, 639798 Singapore*

Abstract

The abundant occurrence of calcium carbonate minerals in marine sediments and their high fluorine content suggests that fluorine is a good candidate for reconstructing paleoceanographic parameters. However, the potential of fluorine as a paleoproxy had hardly been explored, and fundamental insights into the behaviour of fluorine in biogenic carbonates and marine sediments is required. A first-principles modelling approach is used here to analyse the incorporation mechanisms of fluorine into crystalline calcium carbonates. We compute F incorporation into the CaCO_3 lattice via a number of mechanisms, but concentrate on comparison of the energetics of the two easiest substitution mechanisms: replacing one oxygen atom within the carbonate group to form a $(\text{CO}_2\text{F})^-$ group as against a substitution involving replacement of the CO_3 group by two fluorine ions to form a CaF_2 defect. These incorporation mechanisms are fundamentally different from that of iodine into calcium carbonates, where a carbon atom is replaced. Our simulations suggest that the substitution of CO_3^{2-} by F_2^{2-} is the most favoured and that fluorine is preferentially incorporated into the three naturally-occurring polymorphs of calcium carbonate in the order vaterite \gtrsim

*Corresponding authors

Email addresses: zsteiner@geomar.de (Zvi Steiner), simon.redfern@ntu.edu.sg (Simon A. T. Redfern)

aragonite \gg calcite. These results explain the previously-reported preponderance of fluorine in aragonite corals, and lend support to the use of F/Ca as a proxy for ocean $p\text{CO}_2$.

Keywords: first-principles, fluorine, calcium carbonates, F/Ca ratios, marine chemistry

1. INTRODUCTION

Halogens play a number of important roles in the Earth system, both in Earth's ecosystems as well as a key component of many geochemical processes at Earth's surface. For example, they are a major constituent of the oceans, but in addition volcanic emissions of halogens are frequently considerable. Fluorine is unique among the halogens as it is the only such element that is preferentially enriched in Earth's mantle over seawater. The main sink for fluorine in the modern ocean is as an impurity in biogenic calcium carbonates (CaCO_3) and its enrichment in CaCO_3 exceeds chlorine by a factor of 10^5 (Carpenter, 1969). Fluorine concentrations in biogenic aragonites vary between 500 to 1600 ppm (Ramos et al., 2005; Tanaka & Ohde, 2010; Tanaka et al., 2013), making it one of the most abundant impurities in this carbonate mineral phase. Biogenic low-magnesium calcites typically contain 75 to 600 ppm fluorine (Opdyke et al., 1993; Rosenthal & Boyle, 1993), and the fluorine content of biogenic calcites increases as a function of the magnesium content of the calcite (Ohde & Kitano, 1980) (Kendrick, 2018).

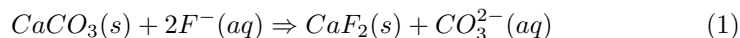
The distinction between the F/Ca ratios of the various CaCO_3 polymorphs, and the large differences between the F/Ca ratio of calcium carbonates and other common fluorine-containing minerals (e.g. fluorapatite and fluorite), suggests the potential of using fluorine concentrations in seawater and CaCO_3 shells to understand past and present ocean environments. This potential has indeed been successfully realised in studies of mineral precipitation and dissolution occurring during early diagenesis in shallow marine sediments (Green & Aller, 2001; Rude & Aller, 1991). In theory, seawater concentrations of fluorine can

25 also be used in studies of global biogeochemistry. For example, Steiner et al.
26 (2014, 2018) demonstrated how variations in seawater concentrations of stron-
27 tium and calcium can be used to quantify the contributions of coral reefs and
28 pelagic plankton to the CaCO_3 cycle of the Red Sea, based on the tendencies of
29 various groups of calcareous organisms to incorporate strontium into their skele-
30 tons. Since fluorine concentrations also vary between skeletons precipitated by
31 different groups of organisms, measurements of seawater concentrations of flu-
32 orine can be used to improve our understanding of the marine CaCO_3 cycle of
33 the modern ocean and, for example, monitor the effects of ocean acidification
34 on various groups of organisms.

35 Despite the promising prospect fluorine offers for marine sciences and pa-
36 leoceanographic studies, alongside the fact that the fluorine concentrations in
37 CaCO_3 shells are relatively high, the application of fluorine concentrations as
38 indicators in environmental studies is very limited at present. The main reason
39 for this is that the mechanism by which fluorine is incorporated into CaCO_3
40 is relatively poorly understood and there are no reliable predictions of how
41 the incorporation of fluorine should change with varying environmental condi-
42 tions. This problem is exemplified by the fact that there is no experimental
43 evidence to show any correlation between the fluorine content of, for example,
44 foraminiferal tests and the surface salinity and temperature of seas in which
45 they grow. Instead, fluorine contents seem to vary according to the preferred
46 depth of calcification of individual foraminifera species (Opdyke et al., 1993;
47 Rosenthal & Boyle, 1993; Rosenthal et al., 1997). A recent study of laboratory-
48 cultured benthic foraminifera suggests that the carbonate ion concentration of
49 the growth medium is the only environmental parameter that co-varies with the
50 fluorine content of foraminifera shells Roepert et al. (2019).

51 Though we cannot rule out the possibility of surface adsorption and intersti-
52 tial site incorporation, there are solid lines of experimental evidence to suggest
53 that the structural incorporation of fluorine into the crystallographic lattice sites
54 of carbonates is dominant, but the incorporation mechanism is unclear and has
55 been the subject of some debate. For example, Carpenter (1969) suggested

56 that fluorine is primarily incorporated into the calcium carbonate crystal struc-
57 ture, and the form in which the fluorine is present is unresolved. The data from
58 Rosenthal & Boyle (1993) support the notion that fluorine occupies lattice sites,
59 although the nature of this substitution and its fundamental controls were not
60 specified. Ohde & Kitano (1980) and Kitano & Okumura (1973) suggested that
61 the incorporation of fluorine into high-Mg calcites might be coupled with the
62 co-precipitation of Mg, while Ichikuni (1979) suggested that the incorporation
63 of fluorine into the crystalline structure of aragonite occurs by substitution of a
64 carbonate ion by two fluorine ions during crystal growth:



65 This substitution balances the charge of the substituting anions and was termed
66 a "CaF₂" substitution. It should be understood, however, that it is not a
67 substitution of fluorite itself, somehow incorporated into the calcium carbonate
68 structure. Rather, the reaction following equation 1 involves the replacement
69 of one CO₃²⁻ oxy-anion in the carbonate structure by two F⁻ anions. The
70 relatively high partition coefficient of fluorine in aragonite (0.54-1.26) suggests
71 that fluorine is likely to be incorporated into aragonite (and possibly other
72 carbonate polymorphs) via some such mechanism, although other simpler ionic
73 substitutions cannot be ruled out.

74 Here, we provide a systematic exploration and examination of potential
75 mechanisms of fluorine substitution into the three common biomineral poly-
76 morphs of calcium carbonate, namely calcite, aragonite and vaterite. We use
77 first-principles quantum mechanical *ab initio* structure calculations to obtain
78 the structural and thermodynamic properties of fluorine-bearing carbonates and
79 to explore the mechanism by which the main polymorphs of CaCO₃ might in-
80 corporate fluorine. Our calculations correspond to conditions of zero pressure
81 and temperature, in common with previous such investigations of carbonates
82 (e.g. Archer et al. (2003)), but are the first step in providing insights into the
83 ground state thermodynamic properties of competing trace element incorpora-
84 tion mechanisms.

85 2. COMPUTATIONAL MODELS AND METHODS

86 2.1. Starting structures of CaCO_3

87 Three common polymorphs of calcium carbonate, CaCO_3 , namely calcite,
88 aragonite and vaterite, are all considered in this work. The starting structures
89 for the computational work on calcite, aragonite and vaterite were those crys-
90 tallising in space groups $R\bar{3}c$, $Pnma$, and Cc respectively. The structures of
91 $R\bar{3}c$ calcite and $Pnma$ aragonite are well-known and indeed were among the
92 first to be identified in the early history of X-ray crystallographic studies. We
93 used the structures from Graf (1961) and De Villiers (1971) as starting points
94 for our calculations. The structure of vaterite is much-debated as it appears
95 to occur in a number of competing metastable polymorphs, and we therefore
96 did not use any of the experimentally-derived structures. We choose, instead,
97 the theoretically calculated Cc structure, containing 12 formula units of CaCO_3
98 per unit cell (Demichelis et al., 2013), for the convenience of making a supercell
99 containing the same number of atoms for all three polymorphs.

100 2.2. Super-cells of CaCO_3

101 The incorporation of fluorine into pure calcium carbonate is treated as an im-
102 purity substitutional defect. Calculations were carried out with periodic bound-
103 ary conditions. Such computational methods demand a balance between having
104 a set of atoms (the simulation box) that is large enough such that the local
105 strains associated with the incorporation of a defect are insignificant at its
106 boundaries, with the constraint that the simulation box needs to be compu-
107 tational tractable in the context that the computational cost can scale as N^3 ,
108 where N is the number of atoms. Thus, in order to have a simulation box large
109 enough that periodically repeating fluorine substitutional defects are sufficiently
110 distant that interactions between them are insignificant, a super-cell containing
111 24 formula units of CaCO_3 (120 atoms) was constructed for each of the poly-
112 morphs. We found that a simulation box (the super-cell) containing 120 atoms
113 was large enough to accommodate any local structural distortion induced by

114 the fluorine, within its periodic boundaries, thus allowing us to model impurity
115 incorporation without periodic boundary effects playing a role.

116 In the case of calcite, a super-cell was chosen that corresponds to four con-
117 ventional hexagonal unit cells. The super-cell was, therefore, constructed as
118 $2a \times 2b \times c$ where a , b , and c are the unit cell parameters of the hexagonal
119 setting of the calcite $R\bar{3}c$ unit cell. For aragonite, the simulation box again con-
120 tained 120 atoms and was comprised of a super-cell six times the volume of the
121 conventional aragonite unit cell, constructed as $2a \times 3b \times c$, where a , b , and c are
122 the unit cell parameters of the orthorhombic $Pnma$ unit cell of aragonite. For
123 vaterite, the simulation box was twice the volume of the conventional vaterite
124 unit cell, with a super-cell constructed as $a \times 2b \times c$, with a , b , and c being the
125 cell parameters of the monoclinic Cc unit cell of vaterite.

126 2.3. Structure of fluorine-bearing $CaCO_3$

127 The periodic models of fluorine-bearing $CaCO_3$ were built, for structural
128 optimisation, by introducing one fluorine atom into the $CaCO_3$ supercell and
129 substituting one atom out, in three different substitution mechanisms. The
130 first involved the substitution of a fluorine atom for calcium (Ca-site), onto the
131 large octahedral site. The second corresponds to the substitution of fluorine for
132 carbon (C-site), as a FO_3^- replacing the carbonate group, as observed in the case
133 of iodine substitution (Podder et al., 2017; Feng & Redfern, 2018). The third
134 involved the substitution of a fluorine atom for oxygen atom (O-site), forming
135 $(CO_2F)^-$ groups. In each case the modified structures correspond to an average
136 site occupancy of around 4% substitution of fluorine onto the site. In addition,
137 we tested the "CaF₂" incorporation mechanism by introducing two fluorines
138 into the structure and substituting this pair of F^- anions for a CO_3^{2-} group,
139 with an initial starting configuration in which each fluorine was placed at the
140 position of one of the three oxygens previously occupied in the carbonate group
141 that had been removed. The substituted structures are constructed without
142 imposing any symmetry restrictions, by starting from a set of atomic positions
143 equivalent to the host phase but with the symmetry then reduced to $P1$, and

144 thus optimised under no symmetry restrictions, which means the full system
145 geometry is relaxed. In many cases, there is more than one way to do the
146 substitution, and all the structures reported here correspond to those with the
147 lowest energies, having tested each option.

148 2.4. Structural optimisation

149 The energetics and physical properties of pure carbonates and fluorine-
150 substituted phases were calculated using first-principles methods based on den-
151 sity functional theory, using periodic boundary conditions. Calculations are per-
152 formed employing the Vienna *ab initio* simulation package (Kresse & Furthmüller,
153 1996). A kinetic energy cut-off of 520 eV was chosen after testing to ensure that
154 it was large enough to arrive at converged reliable energies to less than 1 meV.
155 Monkhorst-Pack meshes for Brillouin zone sampling were selected with a res-
156 olution of 0.3 \AA^{-1} (see Supplementary Materials, Fig. S1). The generalised
157 gradient approximation (Perdew et al., 1992) in the scheme of the Perdew-
158 Burke-Enzerhoff (Perdew et al., 1996) pseudo-potentials was used, alongside
159 projected-augmented-wave (PAW) potentials (Perdew et al., 1992, 1996) for
160 electron-ion interactions. PAW potentials with $3s^23p^64s^2, 2s^22p^2, 2s^22p^4,$ and
161 $2s^22p^5$ electrons as valence electrons were adopted for the Ca, C, O and F
162 atoms respectively.

163 We checked one set of F defect calculations against the energies of the pure
164 (F-free) system to confirm whether dispersion corrections are required. The re-
165 sults of the three sets of calculations are listed in the Supplementary Materials
166 (Table S1). Focusing on the O-site substitution, for example, we get the results
167 as in Table S2, which demonstrate influence of dispersion corrections on our
168 observations and we find it does not impact the relative enthalpy differences
169 seen. With or without dispersion correction we still see that the relative en-
170 thalpies of vaterite < aragonite \ll calcite for the $(\text{CO}_2\text{F})^-$ group substitution
171 are not affected and the introduction of dispersion corrections does not change
172 our conclusions.

173 Note that the calculations do not assume the oxidation state of the halogen

Table 1: Energy increases (relative to pure components) due to fluorine incorporation in CaCO_3 , calculated according to reactions 2, 3, 4 and 5. Units are kJ/mol (CaCO_3).

phase	Ca-site substitution	FO_3 defect	CO_2F defect	CaF_2 defect
calcite	42.13	40.47	13.22	-12.08
aragonite	41.37	39.09	7.57	-14.59
vaterite	35.82	32.53	5.56	-15.08

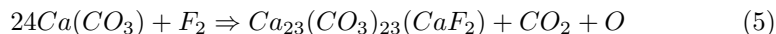
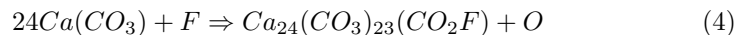
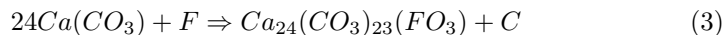
174 or other elements, but simply find the lowest enthalpy configuration based on the
 175 pseudo-potential model. Atomic relaxations were terminated when the change
 176 of the total energy per atom converged to within 1 meV per atom. All the
 177 calculations were conducted at ambient pressure and 0 K, which provides an in-
 178 sight into the ground state energies of the competing incorporation mechanisms.
 179 Crystal structures were plotted using VESTA, a programme for 3D visualisation
 180 of crystal structures and volumetric data (Momma & Izumi, 2011).

181 3. RESULTS

182 3.1. Enthalpies of fluorine-doped calcium carbonates

183 Using the relaxed structures as a starting point, the properties of fluorine-
 184 doped equivalents have been calculated either by introducing one fluorine atom
 185 into each of the supercells in the three substitution mechanisms specified by
 186 reactions 2, 3, and 4 below, or by introducing two fluorine atoms in place of the
 187 a carbonate group, following reaction 5. From the results of the calculations
 188 of energies, at zero temperature and pressure, of each of the relaxed structures
 189 fluorine-free and fluorine-bearing calcium carbonate structures, combined with
 190 the energies for elemental Ca, C, O and F under the same conditions, the ener-
 191 gies associated with substitutional fluorine incorporation were determined. The
 192 following substitution schemes for all the three polymorphs (calcite, aragonite
 193 and vaterite) of CaCO_3 explain where the F is placed in the structure of cal-
 194 cite (it is important to understand that these equations are merely intended to

195 explain where the F is placed in the structure of calcite, and do not necessarily
 196 represent realistic substitution reactions):



197 Incorporation of fluorine in calcium carbonates by the first three of these
 198 mechanisms is associated with some charge imbalance. In our calculations we
 199 have assumed a homogeneous electrostatic background. This corresponds to
 200 a mean field approach and, indeed, charge compensation may occur via sub-
 201 stitutions that act over across much larger distances than those of our mod-
 202 elling simulation cell (including compensation at free surfaces). Given the very
 203 large number of possible coupled substitution mechanisms we have chosen not
 204 to attempt to explore individual potential mechanisms. The assumption of a
 205 homogeneous electrostatic background leads to reasonable description of the
 206 atomic-scale environment of the impurity, which is our main interest.

207 Calculated enthalpies for each of the reactants and products allow us to
 208 determine the reaction energies, at zero temperature and pressure, for each of
 209 these schemes in each of the three $CaCO_3$ polymorphs. The energies of these four
 210 reactions, calculated thus, are listed in Table 1. The energies associated with flu-
 211 orine incorporation, as suggested by the calculation of the energies of $(CO_2F)^-$
 212 defect and CaF_2 defect substituted compounds, for all three polymorphs, are
 213 significantly lower than the energies associated with Ca-site and C-site (or, FO_3
 214 defect) fluorine substitutions. This result is very different from findings for io-
 215 dine substitution into carbonates, where iodine is most easily accommodated

216 into calcium carbonates via C-site substitution, forming an iodate oxyanion
217 group, IO_3^- , replacing the carbonate group (Feng & Redfern, 2018). It has pre-
218 viously been seen that reaction of fluorine ions with CO_2 to form $(\text{CO}_2\text{F})^-$ is
219 energetically feasible and has been experimentally observed (Bhargava & Bala-
220 subramanian, 2007), suggesting that such $(\text{CO}_2\text{F})^-$ groups are indeed realistic
221 species for potential incorporation into carbonates and that they might well be
222 available in seawater for uptake by calcifying organisms. The substitution of
223 two fluorine atoms onto two oxygen positions, and removal of the entire asso-
224 ciated CO_3 group, is, however, even more favourable in our calculations. We
225 find that the incorporation of this "CaF₂ defect", becomes exothermic and is
226 significantly lower than the enthalpy of reaction of the $(\text{CO}_2\text{F})^-$ substitution
227 scheme for calcite, aragonite and vaterite. For both of these two lower-energy
228 reaction schemes we find that substitution of fluorine into vaterite is slightly
229 more easily accommodated than in aragonite, but that substitution of fluorine
230 into calcite is far more difficult, indicated by the higher enthalpy of substitution.

231 Our calculations give the enthalpies of each of the structures of interest,
232 that is, each of the tested modes of fluorine incorporation into calcite, arag-
233 onite and vaterite, relative to the fluorine-free equivalents. This provides the
234 thermodynamic baseline against which geochemical incorporation mechanisms
235 may be understood. Of course, each incorporation mechanism will, at elevated
236 temperature, be associated with a further reduction in Gibbs energy due to en-
237 tropic effects. Comparing the four reactions listed above we see that reactions
238 2 (Ca-F substitution) and 3 (C-F substitution) will be lower in entropy than
239 reactions 4 and 5 (one, or two, F atom(s) replacing oxygen in the carbonate
240 group, with or without removal of the remaining O and C atoms) since, for
241 reactions 2 and 3 there is only one way to do the substitution, there being only
242 one Ca or C in the formula unit, whereas for reactions 4 and 5 there are three
243 ways (in each case) to replace either one or two out of three oxygen atoms in the
244 carbonate group. Thus, entropic effects are also likely to favour both CO_2F and
245 CaF_2 defect substitution over Ca-site substitution or FO_3 defects. Furthermore,
246 the configurational entropies associated with CO_2F and CaF_2 substitutions are

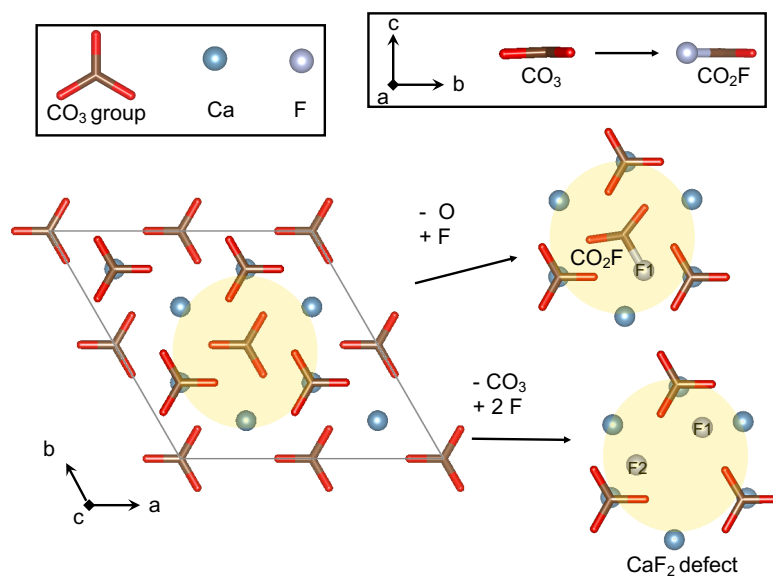


Figure 1: Minimum energy structure of calcite, with an indication of the local structure around a fluorine-bearing defect at the position indicated by the yellow shading for the CO_2F and CaF_2 substitutions. The solid lines around the structure mark the bounds of the simulation box.

247 expected to be similar.

248 3.2. Structural distortion

249 The incorporation of fluorine into each of the calcium carbonate polymorphs
 250 induces local structural distortion in the lattice around the incorporated atoms
 251 to some extent, breaking down the local symmetry of the host structures (Fig-
 252 ures 1,2, and 3). The symmetries of the resultant structures have been analysed
 253 and are summarised in Table 2. It is found that they are $C2$ for CO_2F -bearing
 254 calcite, Pm for the CO_2F -bearing aragonite, which is the same as was found
 255 for iodine-substituted aragonite by Feng & Redfern (2018), and $P1$ for CO_2F -
 256 bearing vaterite. It should be stressed that we are not suggesting that halogen
 257 substitution at the ppm level, as seen in nature, would result in reduction of

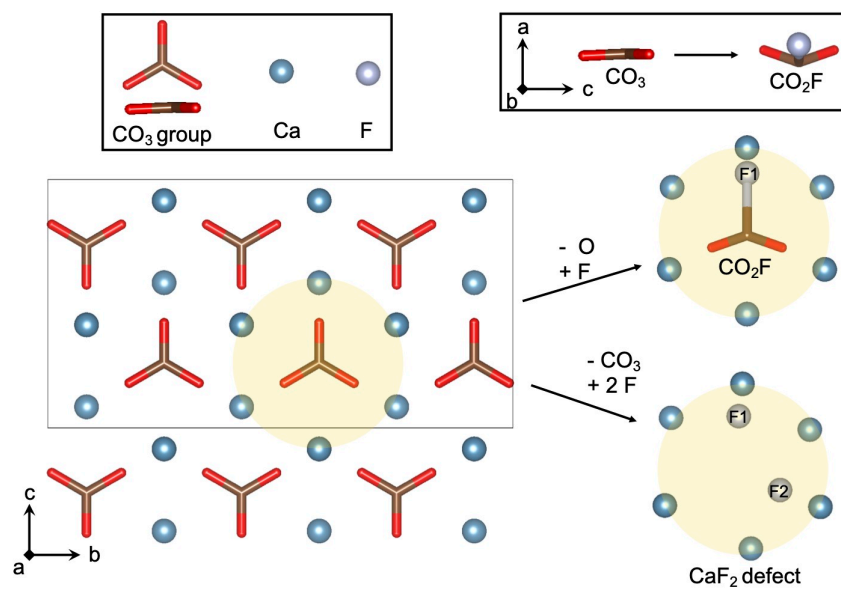


Figure 2: Minimum energy structure of aragonite, with an indication of the local structure around a fluorine-bearing defect at the position indicated by the yellow shading for the CO_2F and CaF_2 substitutions. The solid lines around the structure mark the bounds of the simulation box.

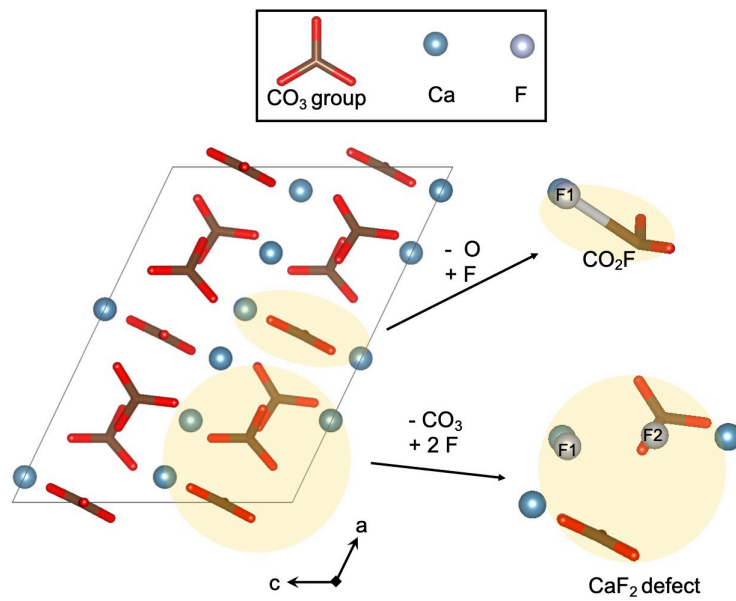


Figure 3: Minimum energy structure of calcite, with an indication of the local structure around a fluorine-bearing defect at the position indicated by the yellow shadings for the CO_2F and CaF_2 substitutions. The solid lines around the structure mark the bounds of the simulation box.

Table 2: Analysis of the structural distortions of CaCO_3 phases arising from incorporation of a CO_2F defect, with a comparison to those of the CaF_2 - defect type incorporation and of pure calcium carbonates.

Phase	Space group	Volume (\AA^3)	Bond length (\AA)		
			C-F	C- $\text{O}_{\text{CO}_2\text{F}}$	C- O_{CO_3}
CO_2F -bearing calcite	$C2$	366.3	2.08	1.26	1.29-1.30
CaF_2 -bearing calcite	$C2$	381.4	-	-	
calcite	$R\bar{3}c$	381.5	-	-	
CO_2F -bearing aragonite	Pm	223.0	2.08	1.26	1.29-1.30
CaF_2 -bearing aragonite	$P1$	233.6	-	-	
aragonite	$Pnma$	233.5	-	-	
CO_2F -bearing vaterite	$P1$	745.8	2.58	1.25	1.28-1.31
CaF_2 -bearing vaterite	$P1$	775.8	-	-	
vaterite	Cc	782.4	-	-	

258 the long-range space group symmetry of a carbonate host crystal to these sym-
 259 metries. Rather, these represent the symmetry of the local distortion that is
 260 to be expected around a halogen substituent atom when hosted within the ma-
 261 trix of such a phase. It appears that, in order to accommodate fluorine atoms
 262 by substitution of $(\text{CO}_3)^{2-}$ by $(\text{CO}_2\text{F})^-$, the lattice becomes slightly smaller,
 263 with a small reduction in molar volume. The volumes of CO_2F -bearing and
 264 CaF_2 -bearing carbonate unit cells are give in Table 2 from which it can be seen
 265 that the incorporation of fluorine by the CaF_2 -type defect occurs with almost
 266 no change in density, or unit cell volume, in the case of calcite and aragonite,
 267 with the two F^- anions that replace the CO_3^{2-} group taking up almost identical
 268 space in the carbonate site position.

269 4. DISCUSSION

270 4.1. Structural incorporation

271 Experimental observations suggest that fluorine is not simply adsorbed onto
 272 calcium carbonate surfaces, but instead is incorporated into the CaCO_3 crystal

273 structure (Carpenter, 1969). Ichikuni (1979) carried out further studies of the
274 uptake of F^- in aragonite which indicated that fluorine is associated with struc-
275 tural incorporation into aragonite and suggested that one $(CO_3)^{2-}$ is replaced
276 by two F^- ions, co-precipitating with Ca^{2+} to form CaF_2 .

277 Approximately half of the fluorine in seawater occurs in the form of molecular
278 complexes, principally as MgF^+ ion pairs. For the remainder, fluorine, due
279 to its high electronegativity, occurs as free anions (F^-). Clearly one possible
280 substitution mechanism corresponds to that in which one CO_3^{2-} oxy-anion in
281 calcium carbonate is replaced by two F^- ions, as suggested earlier by Ichikuni
282 (1979). Here, we have also explored other possible incorporation mechanisms.
283 We rule out co-precipitating with Ca^{2+} to nucleate and grow discrete crystalline
284 precipitates of CaF_2 since fluorite (CaF_2) is undersaturated in seawater and such
285 a complex is unlikely to precipitate (Sillén, 1961). Secondly, the structure of
286 fluorite is very different from that of the calcium carbonate polymorphs, and
287 the mismatch in structure means that the interface energy of any precipitate
288 would be high, such that nucleation and growth of precipitates of fluorite would
289 be inhibited. Furthermore, Ichikuni (1979) reported that fluoride in aragonites
290 precipitated from controlled aqueous solutions was homogeneously distributed,
291 with no indication of discrete fluorite precipitates.

292 In all three polymorphs (calcite, aragonite and vaterite), when we compare
293 a single atom of fluorine substituting onto the Ca-site, C-site or O-site, we
294 find that substitution of fluorine for oxygen (forming a $(CO_2F)^-$ complex) is
295 the most favoured. This is in contrast to the behaviour of iodine, which favours
296 substitution onto the C-site to form an iodate molecule in terms of incorporation
297 mechanism (Feng & Redfern, 2018). The formation of $(CO_2F)^-$ groups within
298 carbonate is not entirely surprising, in view of the earlier work of Bhargava &
299 Balasubramanian (2007). It was found that, in reaction between fluorine and
300 carbon dioxide, fluorine anions react with CO_2 to form $(CO_2F)^-$ groups, with
301 one consequence of this reaction being the distortion of the CO_2 molecule away
302 from linearity (Bhargava & Balasubramanian, 2007). We find a similar molec-
303 ular configuration in our simulations of carbonates adopting this substitution

304 mechanism. By extending the extent of substitution from one fluorine replacing
305 oxygen at the carbonate group, to two fluorines replacing two carbonate oxy-
306 gens and removal of the remaining oxygen and carbon atoms (the mechanism
307 proposed by Ichikuni (1979) for aragonite) we arrive at an even more favoured
308 fluorine incorporation mechanism. Not only does this process result in twice
309 the amount of fluorine incorporated per defect, the energetics of the substitu-
310 tion reaction, reaction 5, are significantly smaller than the other mechanisms
311 that we investigated.

312 Our simulations demonstrate that there are significant differences between
313 the defect energies of the fluorine-bearing carbonate polymorphs. We find that
314 the energy associated with incorporation of fluorine into calcite is the greatest
315 of the three polymorphs, with incorporation of fluorine into aragonite and va-
316 terite being much more favourable (Table 1). We note that our discussion is
317 focussed entirely on thermodynamic considerations. For biogenic carbonates,
318 non-equilibrium effects, such as those associated with cell metabolism, may
319 also play significant roles in element incorporation. However, as discussed be-
320 low, our results, based purely on the ground state thermodynamic properties of
321 these structures, are reflected in observations of geochemical trends in natural
322 systems, underlining the importance of equilibrium as a baseline consideration.

323 We conclude that fluorine will partition much more strongly into aragonite
324 than into calcite. Comparing incorporation of fluorine into the three naturally-
325 occurring polymorphs of calcium carbonate (including the metastable vaterite
326 polymorph) we find that fluorine is expected to enter each polymorph with
327 relative concentrations in the the order of vaterite \gtrsim aragonite \gg calcite. This
328 finding is in agreement with the observations (on natural samples) of Carpenter
329 (1969) who found that aragonites show much higher fluorine concentrations than
330 calcites. The relative ease with which vaterite accommodates both the CO_2F
331 and the CaF_2 defect does, however, raise the possibility of biogenic incorporation
332 of fluorine into calcite via inheritance from a vaterite precursor. We note, for
333 example, that Jacob et al. (2017) proposed that foraminiferal calcite forms via
334 precursor vaterite, in the early stages of calcification. Given this, one might

335 expect that the stable “daughter” calcite forming the organism’s shell may well
336 reflect the partitioning, under biological calcification, set by that of the parent
337 vaterite crystals.

338 *4.2. Insights into ocean chemistry*

339 The evidence of the uptake of fluorine by calcium carbonate is clear, and we
340 have identified the likely mechanism of uptake. The earlier observations that
341 aragonite is able to accommodate fluorine much more easily than calcite are
342 born out in our results. Furthermore, the ion exchange reaction outlined in
343 equation 1 is indeed confirmed as the most favourable route to incorporation.
344 As a consequence, our results lend further support to the idea that the fluorine
345 content of biogenic carbonates may be employed as a good indicator of the
346 partial pressure of CO₂ ($p\text{CO}_2$) in the oceans, and hence of the impacts of
347 changes in atmospheric carbon dioxide. Since equation 1 (equivalent to reaction
348 5 in our schemes) is an exchange reaction, it implies that fluorine in carbonate
349 will have sensitivity to $p\text{CO}_2$, since increases in $p\text{CO}_2$ will result in reductions
350 in pH and carbonate ion concentration ($[\text{CO}_3^{2-}]$) in seawater, which should
351 result in an increase in fluorine concentration, measured in biogenic carbonates
352 as F/Ca, in agreement with the results of Roepert et al. (2019). While we can
353 expect this to be the dominant control on fluorine contents in biogenic calcium
354 carbonates in the oceans, especially given this reaction incorporates two fluorine
355 atoms into the structure, we also note that reaction 4, which is only slightly
356 more exothermic, implies F in carbonate should have some sensitivity to $p\text{O}_2$ in
357 seawater. This would imply an expected correlation between iodine (a redox-
358 sensitive geochemical tracer in biogenic carbonates) and fluorine in carbonates.

359 **5. CONCLUSIONS**

360 The incorporation of fluorine into all three naturally-occurring polymorphs
361 of calcium carbonate – calcite, aragonite and vaterite, has been investigated
362 via first-principles computational methods. In each case the incorporation of a

363 fluorine atom is favoured most strongly as substituent of two fluorine ions for
364 a carbonate, forming a CaF_2 defect. However, substitution of one fluorine for
365 one oxygen in the form of $(\text{CO}_2\text{F})^-$ groups, which causes local distortions of the
366 structure over a length scale of around 10 \AA , is also relatively easy, although not
367 favoured to the extent of the CaF_2 defect. The incorporation of fluorine into
368 vaterite is easiest, for all substitution mechanisms, although only marginally so
369 for the CaF_2 and $(\text{CO}_2\text{F})^-$ defects compared with incorporation into aragonite.
370 Both aragonite and vaterite can, however, accommodate fluorine much more
371 easily than the expected uptake of fluorine into calcite. These findings are sup-
372 ported by the experimentally observed trends in the distribution coefficients for
373 fluorine into CaCO_3 , which are larger for aragonite than for calcite. They are
374 also consistent with the earlier experimental observations of fluorine incorpora-
375 tion into aragonite, lending further support to the idea that F/Ca , especially in
376 biogenic aragonite (e.g. corals), can be used as a reliable proxy for ocean $p\text{CO}_2$,
377 providing a further route for measurement of past changes in atmospheric CO_2
378 and associated paleoclimatic variations.

379 **DATA AVAILABILITY**

380 Research Data associated with this article can be access at:
381 Figshare <https://doi.org/10.6084/m9.figshare.11858160.v1>

382 **AUTHOR CONTRIBUTIONS**

383 XF, ZS and SATR initialised the idea of this study during conversations
384 over coffee in the common room of the Department of Earth Sciences, Downing
385 Street, Cambridge. XF conducted the calculations and interpreted the data.
386 XF, ZS and SATR analysed results and wrote the manuscript together.

387 **COMPETING INTERESTS**

388 The authors declare no competing interests.

389 **ACKNOWLEDGEMENT**

390 XF acknowledges the financial support from Chinese Scholarship Council
391 and from NERC via grant NE/P012167/1. The authors are grateful for con-
392 structive comments from two anonymous reviewers and from Mark Kendrick
393 which greatly improved the manuscript.

394 **References**

- 395 Archer, T., Birse, S., Dove, M., Redfern, S., Gale, J., & Cygan, R. (2003). An
396 interatomic potential model for carbonates allowing for polarization effects.
397 *Physics and Chemistry of Minerals*, 30. doi:10.1007/s00269-002-0269-z.
- 398 Bhargava, B., & Balasubramanian, S. (2007). Probing anion-carbon diox-
399 ide interactions in room temperature ionic liquids: Gas phase cluster
400 calculations. *Chemical Physics Letters*, 444, 242 – 246. URL: <http://www.sciencedirect.com/science/article/pii/S0009261407009803>.
401 doi:<https://doi.org/10.1016/j.cplett.2007.07.051>.
- 403 Carpenter, R. (1969). Factors controlling the marine geochemistry of
404 fluorine. *Geochimica et Cosmochimica Acta*, 33, 1153–1167. URL:
405 <https://linkinghub.elsevier.com/retrieve/pii/0016703769900386>.
406 doi:10.1016/0016-7037(69)90038-6.
- 407 De Villiers, J. P. R. (1971). Crystal structures of aragonite , strontianite , and
408 witherite. *The American Mineralogist*, 56, 758–767.
- 409 Demichelis, R., Raiteri, P., Gale, J. D., & Dovesi, R. (2013). Examining the
410 accuracy of density functional theory for predicting the thermodynamics of
411 water incorporation into minerals: The hydrates of calcium carbonate. *Jour-
412 nal of Physical Chemistry C*, 117, 17814–17823. doi:10.1021/jp4048105.
- 413 Feng, X., & Redfern, S. (2018). Iodate in calcite, aragonite and va-
414 terite CaCO₃: Insights from first-principles calculations and implica-
415 tions for the I/Ca geochemical proxy. *Geochimica et Cosmochimica*

416 *Acta*, . URL: [https://www.sciencedirect.com/science/article/pii/](https://www.sciencedirect.com/science/article/pii/S0016703718300875)
417 S0016703718300875. doi:10.1016/J.GCA.2018.02.017.

418 Graf, D. L. (1961). Crystallographic tables for the rhombohedral carbonates.
419 *American Mineralogist*, 46, 1283–1316.

420 Green, M. A., & Aller, R. C. (2001). Early diagenesis of calcium carbonate in
421 Long Island Sound sediments: Benthic fluxes of Ca²⁺ and minor elements
422 during seasonal periods of net dissolution. *Journal of Marine Research*,
423 59, 769–794. URL: [http://www.ingentaselect.com/rpsv/cgi-bin/](http://www.ingentaselect.com/rpsv/cgi-bin/cgi?ini=xref{&}body=linker{&}reqdoi=10.1357/002224001762674935)
424 [cgi?ini=xref{&}body=linker{&}reqdoi=10.1357/002224001762674935.](http://www.ingentaselect.com/rpsv/cgi-bin/cgi?ini=xref{&}body=linker{&}reqdoi=10.1357/002224001762674935)
425 doi:10.1357/002224001762674935.

426 Ichikuni, M. (1979). Uptake of fluoride by aragonite. *Chemical Geol-*
427 *ogy*, 27, 207–214. URL: [https://linkinghub.elsevier.com/retrieve/](https://linkinghub.elsevier.com/retrieve/pii/0009254179900391)
428 [pii/0009254179900391](https://linkinghub.elsevier.com/retrieve/pii/0009254179900391). doi:10.1016/0009-2541(79)90039-1.

429 Jacob, D. E., Wirth, R., Agbaje, O. B., Branson, O., & Eggins, S. M. (2017).
430 Planktic foraminifera form their shells via metastable carbonate phases. *Na-*
431 *ture Communications*, 8. doi:10.1038/s41467-017-00955-0.

432 Kendrick, M. A. (2018). Halogens in seawater, marine sediments and the altered
433 oceanic lithosphere. In *The role of halogens in terrestrial and extraterrestrial*
434 *geochemical processes* (pp. 591–648). Springer.

435 Kitano, Y., & Okumura, M. (1973). Coprecipitation of fluoride with calcium
436 carbonate. *Geochemical Journal*, 7, 37–49.

437 Kresse, G., & Furthmüller, J. (1996). Efficient iterative schemes for ab initio
438 total-energy calculations using a plane-wave basis set. *Physical Review B*,
439 54, 11169–11186. URL: [https://link.aps.org/doi/10.1103/PhysRevB.](https://link.aps.org/doi/10.1103/PhysRevB.54.11169)
440 [54.11169](https://link.aps.org/doi/10.1103/PhysRevB.54.11169). doi:10.1103/PhysRevB.54.11169. arXiv:0927-0256(96)00008.

441 Momma, K., & Izumi, F. (2011). Vesta 3 for three-dimensional visualization of
442 crystal, volumetric and morphology data. *Journal of applied crystallography*,
443 44, 1272–1276.

- 444 Ohde, S., & Kitano, Y. (1980). Incorporation of fluoride into Ca-Mg
445 carbonate. *Geochemical Journal*, *14*, 321–324. URL: [http://joi.jlc.
446 jst.go.jp/JST.Journalarchive/geochemj1966/14.321?from=CrossRef](http://joi.jlc.jst.go.jp/JST.Journalarchive/geochemj1966/14.321?from=CrossRef).
447 doi:10.2343/geochemj.14.321.
- 448 Opdyke, B. N., Walter, L. M., & Huston, T. J. (1993). Fluoride
449 content of foraminiferal calcite: Relations to life habitat, oxygen
450 isotope composition, and minor element chemistry. *Geology*,
451 *21*, 169. URL: [https://pubs.geoscienceworld.org/geology/article/
452 21/2/169-172/186463](https://pubs.geoscienceworld.org/geology/article/21/2/169-172/186463). doi:10.1130/0091-7613(1993)021<0169:FCOFCR>
453 2.3.CO;2.
- 454 Perdew, J. J. P., Burke, K., & Ernzerhof, M. (1996). Generalized Gra-
455 dient Approximation Made Simple. *Physical Review Letters*, *77*, 3865–
456 3868. URL: <https://link.aps.org/doi/10.1103/PhysRevLett.77.3865>.
457 doi:10.1103/PhysRevLett.77.3865. arXiv:0927-0256(96)00008.
- 458 Perdew, J. P., Chevary, J. A., Vosko, S. H., Jackson, K. A., Pederson, M. R.,
459 Singh, D. J., & Fiolhais, C. (1992). Applications of the generalized gradient
460 approximation for exchange and correlation. *Phys Rev B*, *46*, 6671–6687.
461 doi:10.1103/PhysRevB.46.6671.
- 462 Podder, J., Lin, J., Sun, W., Botis, S. M., Tse, J., Chen, N., Hu, Y., Li, D.,
463 Seaman, J., & Pan, Y. (2017). Iodate in calcite and vaterite: Insights from
464 synchrotron X-ray absorption spectroscopy and first-principles calculations.
465 *Geochimica et Cosmochimica Acta*, *198*, 218–228. doi:10.1016/j.gca.2016.
466 11.032.
- 467 Ramos, A. A., Ohde, S., Hossain, M. M. M., Ozaki, H., Sirirattanachai, S.,
468 & Apurado, J. L. (2005). Determination of fluorine in coral skeletons by
469 instrumental neutron activation analysis. *Journal of Radioanalytical and Nu-
470 clear Chemistry*, *266*, 19–29. URL: [http://link.springer.com/10.1007/
471 s10967-005-0863-x](http://link.springer.com/10.1007/s10967-005-0863-x). doi:10.1007/s10967-005-0863-x.

- 472 Roepert, A., Polerecky, L., Geerken, E., Reichart, G.-J., & Middel-
473 burg, J. J. (2019). Distribution of chlorine and fluorine in benthic
474 foraminifera. *Biogeosciences Discussions*, 2019, 1–27. URL: [https://www.
475 biogeosciences-discuss.net/bg-2019-424/](https://www.biogeosciences-discuss.net/bg-2019-424/). doi:10.5194/bg-2019-424.
- 476 Rosenthal, Y., & Boyle, E. A. (1993). Factors controlling the flu-
477 oride content of planktonic foraminifera: An evaluation of its pa-
478 leoceanographic applicability. *Geochimica et Cosmochimica Acta*,
479 57, 335–346. URL: [https://linkinghub.elsevier.com/retrieve/pii/
480 001670379390435Y](https://linkinghub.elsevier.com/retrieve/pii/S001670379390435Y). doi:10.1016/0016-7037(93)90435-Y.
- 481 Rosenthal, Y., Boyle, E. A., & Slowey, N. (1997). Temperature control
482 on the incorporation of magnesium, strontium, fluorine, and cadmium
483 into benthic foraminiferal shells from Little Bahama Bank: Prospects
484 for thermocline paleoceanography. *Geochimica et Cosmochimica Acta*,
485 61, 3633–3643. URL: [https://linkinghub.elsevier.com/retrieve/pii/
486 S0016703797001816](https://linkinghub.elsevier.com/retrieve/pii/S0016703797001816). doi:10.1016/S0016-7037(97)00181-6.
- 487 Rude, P. D., & Aller, R. C. (1991). Fluorine mobility during early
488 diagenesis of carbonate sediment: An indicator of mineral transfor-
489 mations. *Geochimica et Cosmochimica Acta*, 55, 2491–2509. URL:
490 <https://linkinghub.elsevier.com/retrieve/pii/001670379190368F>.
491 doi:10.1016/0016-7037(91)90368-F.
- 492 Sillén, L. G. (1961). The physical chemistry of seawater. *Oceanography*, .
- 493 Steiner, Z., Erez, J., Shemesh, A., Yam, R., Katz, A., & Lazar, B. (2014).
494 Basin-scale estimates of pelagic and coral reef calcification in the Red
495 Sea and Western Indian Ocean. *Proceedings of the National Academy of
496 Sciences*, 111, 16303–16308. URL: [http://www.pnas.org/lookup/doi/10.
497 1073/pnas.1414323111](http://www.pnas.org/lookup/doi/10.1073/pnas.1414323111). doi:10.1073/pnas.1414323111.
- 498 Steiner, Z., Turchyn, A. V., Harpaz, E., & Silverman, J. (2018). Water chem-
499 istry reveals a significant decline in coral calcification rates in the southern

- 500 Red Sea. *Nature Communications*, 9, 3615. URL: [http://www.nature.com/](http://www.nature.com/articles/s41467-018-06030-6)
501 [articles/s41467-018-06030-6](http://www.nature.com/articles/s41467-018-06030-6). doi:10.1038/s41467-018-06030-6.
- 502 Tanaka, K., & Ohde, S. (2010). Fluoride in coral aragonite related
503 to seawater carbonate. *Geochemical Journal*, 44, 371–378. URL:
504 [http://jlc.jst.go.jp/DN/JST.JSTAGE/geochemj/1.0079?lang=](http://jlc.jst.go.jp/DN/JST.JSTAGE/geochemj/1.0079?lang=en&from=CrossRef&type=abstract)
505 [en&from=CrossRef&type=abstract](http://jlc.jst.go.jp/DN/JST.JSTAGE/geochemj/1.0079?lang=en&from=CrossRef&type=abstract). doi:10.2343/geochemj.1.0079.
- 506 Tanaka, K., Ono, T., Fujioka, Y., & Ohde, S. (2013). Fluoride in
507 non-symbiotic coral associated with seawater carbonate. *Marine Chem-*
508 *istry*, 149, 45–50. URL: [https://linkinghub.elsevier.com/retrieve/](https://linkinghub.elsevier.com/retrieve/pii/S0304420312001399)
509 [pii/S0304420312001399](https://linkinghub.elsevier.com/retrieve/pii/S0304420312001399). doi:10.1016/j.marchem.2012.12.004.